

# MiR-590-5p regulates cell proliferation, apoptosis, migration and invasion in oral squamous cell carcinoma by targeting *RECK*

Wei-Wei Bao, You-Ling Shi, Yan Ma, Xing-Hui Qu, Guang-Ming Pang and Lei Yang

Department of Orthodontics, Dongfeng Stomatological Hospital, Hubei University of Medicine, Shiyan, Hubei Province, China

**Summary.** Objective. To discover the role of miR-590-5p in oral squamous cell carcinoma (OSCC) progression and the corresponding mechanism via the targeting *RECK*.

**Methods.** OSCC (n=85) and normal oral tissues (n=60) were collected to quantify the miR-590-5p expression by using qRT-PCR. Then SCC-15 and OEC-M1 cells were selected and divided into Mock, inhibitor NC, miR-590-5p inhibitor, si-RECK and miR-590-5p inhibitor + si-RECK groups. Dual-luciferase reporter gene assay was used to verify if miR-590-5p could target *RECK*. The biological behaviors of OSCC cells were evaluated by MTT, Wound-healing, Transwell and Flow cytometry. The expression of miR-590-5p and *RECK* was measured by qRT-PCR and Western blotting, respectively.

**Results.** Overexpression of miR-590-5p was found in OSCC tissues. The expression of miR-590-5p was significantly associated with the clinical TNM stage, differentiation degree, and lymph node metastasis of OSCC. *RECK* was identified as a direct target of miR-590-5p. Compared with the Mock group, cells in the miR-590-5p inhibitor group were decreased in terms of proliferation, invasion, and migration, and increased in cell apoptosis, accompanied by down-regulated miR-590-5p, Bcl-2/Bax and MMP-9, and up-regulated *RECK*. By contrast, si-RECK group presented completely opposite changes, and si-RECK reversed the inhibitory effect of miR-590-5p inhibitor on the OSCC cell growth.

**Conclusion.** MiR-590-5p expression was obviously increased in OSCC, and inhibiting miR-590-5p enhanced the expression of its target gene *RECK*, thereby suppressing proliferation, migration and

invasion of OSCC cells and promoting apoptosis of OSCC cells.

**Key words:** MiR-590-5p, *RECK*, Oral squamous cell carcinoma

## Introduction

Oral squamous cell carcinoma (OSCC) is the leading malignant tumor occurring to head and neck, which takes up approximately 5% of all malignancies worldwide (Yang et al., 2015). According to the statistics, there were 28730 new cases and 13805 deaths of oral cancer with approximately 1.3% of all new oral cancer cases and 0.62% of all cancer deaths in 2018 in China (<https://gco.iarc.fr/today/home>). Although the incidence and mortality of oral cancer in China indicated a relatively lower OSCC burden, it attracted much attention and showed a rapid increasing trend since a large number of Chinese are addicted to tobacco and alcohol (Amtha et al., 2014; Zhang et al., 2018). At present, the primary treatment of OSCC is the comprehensive and sequential therapy, namely, surgery supplements by radio-chemotherapy and/or biotherapy (Wikner et al., 2014). The last decades have witnessed great progress made in OSCC treatment, but the high rate of recurrence and metastasis of OSCC limits the overall 5-year survival rate of OSCC patients to only around 50% (Jerjes et al., 2010; Feng et al., 2018). Thus, it is of great significance for the treatment and prognosis improvement of OSCC to understand the pathogenesis of OSCC at the molecular level, and further to explore the potential specific markers related to tumorigenesis (Shiah et al., 2014).

MicroRNAs (miRNAs) refer to the family of single-stranded non-coding RNAs comprised of 18-25 nucleotides (Li et al., 2014). As reported, miRNA can act as an oncogene or a tumor suppresser gene to regulate the growth and metastasis of OSCC cells, thus

*Corresponding Author:* Lei Yang, Department of Orthodontics, Dongfeng Stomatological Hospital, Hubei University of Medicine, No. 16, Daling Road, Zhangwan District, Shiyan 442000, Hubei Province, China. e-mail: yangyyy5@yeah.net  
DOI: 10.14670/HH-18-306



participating in the progression of OSCC (Gombos et al., 2013). Located on long-arm proximal end of chromosome 7 in human genome, miR-590-5p is capable of inhibiting angiogenesis and metastasis of colorectal cancer cells via regulation of NF90/VEGFA signaling pathway (Yang et al., 2013; Zhou et al., 2016). Besides, miR-590-5p possesses the potential to restrict the growth, invasion and migration of osteosarcoma cells through on-target regulation of KLF5 expression (Cai et al., 2018), which could also inhibit the development of tongue cancer by targeting FasL (Xu et al., 2017). Noteworthy, a study found the decreased plasma levels of miR-590-5p in head and neck squamous cell carcinomas (HNSCCs) patients after radio-chemotherapy (Nowicka et al., 2019), demonstrating the controversial of miR-590-5p in oral cancer. As such, we focused our attention mainly on the function of miR-590-5p in OSCC.

Moreover, miR-590-5p was found to regulate the AKT/ERK pathway to affect the growth, invasion and cisplatin sensitivity of GC cells via targeting *RECK* in gastric cancer (GC) cells (Shen et al., 2016). To our knowledge, *RECK* is located on human chromosome 9p13-p12 and widely expressed in the majority of normal tissues and a considerable part of tumor tissues in humans (Liu et al., 2003). As a newly discovered tumor suppressor gene, *RECK* was found reduced in many tumor tissues, such as hepatoblastoma and neuroblastoma (Weaver, 2002; Xu et al., 2015). A previous study revealed a close association between hypermethylation of *RECK* gene and the poor prognosis of OSCC (Long et al., 2008). In addition, *RECK* was suggested to be a prospective prognostic indicator in OSCC since it could prevent the presence of lymphatic metastasis via the imbalance of *RECK* and MMPs (Yuan et al., 2020), and to be a tumor suppressor for the progression of oral cancer in another study (Lin et al., 2020). Given the above, it is reasonable to hypothesize that miR-590-5p may play a regulatory role in OSCC development by specifically modulating the expression of its target gene *RECK*.

In brief, our study was aimed to elucidate the effects of miR-590-5p targeting *RECK* on the biological behaviors of OSCC, thereby laying some theoretical foundation for the early diagnosis and clinical treatment of OSCC.

## Materials and methods

### Ethics statement

Informed consent form was signed by all participants prior to the study. The collection and use of all tissue samples conformed to the relevant ethical principles and was approved by the Ethics Committee of Clinical Experiment of Dongfeng Stomatological Hospital.

### Study subjects

From December 2017 to December 2019, 85 OSCC

patients treated in our hospital were recruited in this study. They were 32-75 years old with the median age 52.3±12.6 years, consisting of 55 males and 30 females. OSCC was diagnosed and classified based on the Tumor Node Metastasis (TNM) system of Unio Internationalis Contra Cancrum (UICC). All patients did not receive radiotherapy, chemotherapy or biological immunotherapy prior to this study. In the meantime, the adjacent non-tumor oral mucosa samples were collected as normal controls from 60 age- and sex-matched patients who received surgical resection for benign tumors during the same period. All the oral mucosa samples were confirmed histologically of normal epithelial cell morphology (without any sign of dysplastic conditions) by pathologists. OSCC tumor tissues and normal tissue samples were preserved in liquid nitrogen for subsequent experiments.

### Cell culturing

Human oral keratinocyte (HOK) (ScienCell, Carlsbad, CA, USA) was cultured in defined keratinocyte-serum free medium (Gibco, NY, USA). Human OSCC cell lines (DOK, FaDu, OC-3, OEC-M1, SCC-4, SCC-9, SCC-15, SCC-25, Tw2.6 and YD-15) were purchased from American type culture collection (ATCC) and cultured in DMEM medium supplemented with 10% inactivated fetal bovine serum (FBS, Gibco), 100 units/mL penicillin (Hyclon) and 100 mg/mL streptomycin (Hyclon), in an incubator of at 37°C with 5% CO<sub>2</sub> (Thermo). When cells covered 80% of the visual field, 0.25% trypsin was used to digest cells for cell passage and subsequent experiments.

### Cell grouping and transfection

SCC-15 and OEC-M1 cells were divided into five groups: Mock group (cells without transfection), inhibitor NC group (cells transfected with negative control sequence of miR-590-5p inhibitor), miR-590-5p inhibitor group (cells transfected with miR-590-5p inhibitor), si-RECK group (cells transfected with *RECK* siRNA), and miR-590-5p inhibitor + si-RECK group (cells co-transfected with miR-590-5p inhibitor and *RECK* siRNA). For cell transfection, SCC-15 and OEC-M1 cells were seeded in 6-well plate and cultured until the cell density reached 70-80%. Then, the transfection was performed according to the instructions of Lipofectamine 2000 (11668-019, Invitrogen, New York, California, USA). Besides, inhibitor NC, miR-590-5p inhibitor and *RECK* siRNA were all purchased from Shanghai GenePharma Co., Ltd.

### Dual-luciferase reporter gene assay

To explore the regulation mechanism of miR-590-5p in affecting *RECK* expression, constructs were generated in which the wild-type (*RECK*-WT) and mutated (*RECK*-MUT) 3'-UTR of *RECK* was inserted downstream of a luciferase reporter. The SCC-15 and

## MiR-590-5p in OSCC via targeting RECK

OEC-M1 cells were co-transfected with RECK-WT or RECK-MUT and miR-590-5p mimic or mimic-NC using Lipofectamine 2000 (Invitrogen, USA). Mimic-NC (negative control) and miR-590-5p mimic were synthesized by Shanghai GenePharma Co., Ltd. After 48 h transfection, cells were collected, split, and detected for luciferase activity according to the instructions on the dual-luciferase reporter assay system (Promega, Madison, WI, USA). The ratio of Firefly to Renilla luciferase activity was regarded as the relative luciferase activity.

### Quantitative reverse transcriptase polymerase chain reaction (qRT-PCR)

Total RNA in tissues and cells was extracted using a miRNeasy Mini Kit (217004, QIAGEN, Germany). Primers designed using the Primer Premier 5.0 software (Premier Biosoft, USA) were synthesized by Takara as follows: miR-590-5p: Forward: 5'-GAGCTTATTCATA AAAGT-3'; Reverse: 5'-TCCACGACACGCAC TGGATACGAC-3'; U6: Forward: 5'-CTCGGCTTCG GCAGCACA-3'; Reverse: 5'-AACGCTTCACGA ATTTGCGT-3'. Reverse Transcriptase M-MLV (D2640A, Takara) was used to synthesize cDNA. After cDNA conversion, the quantity of mature miRNA was evaluated by qRT-PCR performed in obedience to specifications of SYBR<sup>®</sup> Premix Ex Taq<sup>™</sup> II kit (RR820A, TaKaRa). With U6 as the internal reference gene, the relative miR-590-5p expression was calculated using  $2^{-\Delta\Delta C_t}$  method.

### MTT (3-[4, 5-dimethylthiazol-2-yl]-2, 5 diphenyl tetrazolium bromide) method

Cells were collected for cell count, seeded into 96-well plates ( $3 \times 10^3$  cells/well) with 6 replicates, and cultured for 24h, 48h, 72h and 96h, respectively. In the next step, 20  $\mu$ L 5 mg/mL MTT solution (Sigma, USA) was added to each well for 2h of reaction at 37°C. As routine procedures, the upper supernate was discarded and 150  $\mu$ L dimethylsulfoxide (DMSO) was added to each well. Finally, the optical density (OD) at 490 nm was detected by using a spectrophotometric plate reader (Thermo Fisher Scientific).

### Wound-healing assay

Cells were seeded into 6-well plates and cultured with serum-free DMEM medium until cell confluence reached 90-100%. A 10  $\mu$ L pipette was used to vertically draw scratches along the 6-well plate with 4-5 lines across each well. The scratches were consistent in width. Next, cells were washed with serum-free medium to remove floating cells and debris. Then the plate was placed in an incubator for cell culture. At 0 h and 48 h after line scratching, the migrating distance of cells was measured with an inverted microscope and several visual fields were randomly selected for photo taking.

### Transwell invasion assay

Transwell chamber was placed in 24-well plate. Matrigel (1:8 diluted) was used to cover the upper surface of the Transwell chamber bottom before air drying at room temperature. Subsequently, cells were trypsinized, rinsed twice with PBS, suspended in serum-free RPMI 1640 culture medium, and adjusted to cell density  $1 \times 10^5$  cells/mL to prepare cell suspension. In the Matrigel-coated upper chamber, there was 200  $\mu$ L cell suspension, while the lower chamber was occupied by 600  $\mu$ L culture medium filled with 20% FBS. After 24h, Transwell system was taken out to remove detached cells on upper chamber with cotton swabs. Then cells were fixed with 4% Paraformaldehyde for 15 min and stained with 0.5% crystal violet solution (prepared with methanol). Finally, cells were washed with PBS buffer, followed by observation of cell invasion under an inverted microscope (XDS-800D, Shanghai Caikang Optical Instrument Co., Ltd, China), with five randomly selected visual fields being photographed.

### Flow cytometry

At 48h after cell transfection, EDTA-free trypsin was used to digest cells, which were collected in the EP tube for subsequent centrifugation. The upper supernate was discarded. Cells were rinsed with cold PBS buffer for three times, the upper supernate was discarded, and Annexin-V-FITC/PI dye was prepared with Annexin-V-FITC, PI and HEPES (1:2:50) according to the manufacturer's instructions of Annexin-V-FITC cell apoptosis detection kit (Sigma, USA). Next, cells were suspended in the dye by  $1 \times 10^6$  cells/100  $\mu$ L, shaken on an oscillator, cultured for 15 min at room temperature, and mixed with 1 mL HEPES buffer. The fluorescence of FITC and PI was detected to evaluate cell apoptosis, with the wavelength of 488 nm and band pass of excitation wavelength 525 nm and 620 nm, respectively.

### Western blotting

Proteins from the transfected cells were extracted with RIPA buffer (Sigma, USA) and quantified using a BCA kit after cell lysis (Thermo, USA). Electrophoresis with 10% sodium dodecyl sulphate polyacrylamide gel electrophoresis (SDS- PAGE) was used for separation of 40  $\mu$ g proteins, which were transferred to nitrocellulose membrane. After 1h of blocking in 5% skimmed milk at room temperature, blots were then incubated with primary antibodies against RECK (ab211518, Abcam), Bax (ab32503, Abcam), Bcl-2 (ab32124, Abcam), MMP-9 (ab38898, Abcam) and  $\beta$ -actin (ab8226, Abcam) overnight at 4°C. Next, the membrane was washed with PBS (phosphate buffer solution) for three times (5 min each time), followed by incubation at 37°C with the secondary antibody horseradish peroxidase-labeled Goat anti rabbit IgG (1: 1000, Wuhan Boster Biological Technology., LTD, China). Finally, the

membrane was soaked in ECL reaction solution (Pierce, Waltham, MA, USA) for visualization. The gray value ratio of target band to loading control band was considered as the relative expression of target proteins with  $\beta$ -actin as the loading control.

### Statistical methods

Statistical data analysis was conducted using the software SPSS20.0. Measurement data were presented as mean  $\pm$  standard deviation (SD). Difference between two groups was analyzed by student's *t*-test, while comparison among multiple groups tested by One-Way ANOVA followed by Turkey's post hoc test for multiple comparisons.  $P < 0.05$  indicated that the difference is of statistical significance.

### Results

#### MiR-590-5p up-regulation in OSCC tissues and OSCC cell lines

The quantity of mature miRNA for miR-590-5p in OSCC tissues and OSCC cell lines was realized by qRT-PCR. As shown in Figure 1A, miR-590-5p was significantly higher with more than 4-fold increase in OSCC tissues than in normal oral mucosa samples ( $P < 0.001$ ). With human oral keratinocytes (HOK) as baseline for comparison, miR-590-5p expression was remarkably up-regulated in OSCC cells lines DOK (2.85 fold,  $P < 0.001$ ), FaDu (2.52 fold,  $P = 0.003$ ), OC-3 (3.16 fold,  $P < 0.001$ ), OEC-M1 (4.02 fold,  $P < 0.001$ ), SCC-4 (3.16 fold,  $P < 0.001$ ), SCC-9 (2.86 fold,  $P < 0.001$ ), SCC-15 (4.63 fold,  $P < 0.001$ ), SCC-25 (3.74 fold,  $P < 0.001$ ),

Tw2.6 (3.52 fold,  $P < 0.001$ ) and YD-15 (2.92 fold,  $P < 0.001$ ), among which SCC-15, OEC-M1 and SCC-25 cell line had the high levels of miR-590-5p expression (Fig. 1B). Thus, we chose the SCC-15 and OEC-M1 cells for subsequent experiments.

#### Relationship between miR-590-5p expression and clinicopathological characteristics of OSCC patients

As shown in Table 1, miR-590-5p expression was not obviously related to the gender ( $P = 0.517$ ) and age ( $P = 0.809$ ) of OSCC patients, but it was closely

**Table 1.** Relationship between miR-590-5p expression and clinicopathological characteristics of OSCC patients.

Clinicopathological characteristics	N (%)	miR-590-5p	P
<i>Age (Year)</i>			0.517
≤ 60	46 (54.12)	4.90±0.71	
> 60	39 (45.88)	4.80±0.70	
<i>Gender</i>			0.809
Male	55 (64.71)	4.84±0.75	
Female	30 (35.29)	4.80±0.68	
<i>Differentiation degree</i>			<0.001
Well-differentiated	49 (57.65)	4.33±0.44	
Poor-/Moderate-differentiated	36 (42.35)	5.56±0.42	
<i>Clinical stage</i>			<0.001
I-II	47 (55.29)	4.23±0.43	
III-IV	38 (44.71)	5.53±0.43	
<i>Lymph node metastasis</i>			<0.001
With	34 (40.00)	5.59±0.41	
Without	51 (60.00)	4.35±0.46	

P-value is based on student's *t*-test

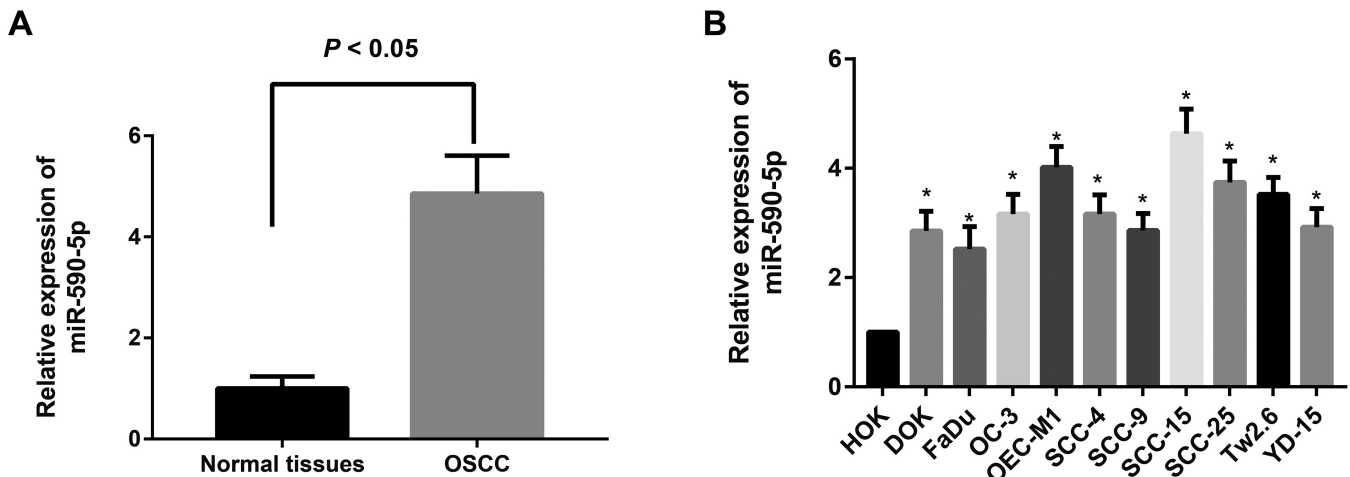


**Fig. 1.** The expression of miR-590-5p in OSCC tissues and OSCC cell lines. **A.** miR-590-5p expression in OSCC tissues ( $n = 85$ ) and normal oral tissues ( $n = 60$ ) quantified by qRT-PCR and statistical analysis was performed with Student's *t*-test; **B.** miR-590-5p expression in human oral keratinocytes (HOK) and OSCC cell lines (DOK, FaDu, OC-3, OEC-M1, SCC-4, SCC-9, SCC-15, SCC-25, Tw2.6 and YD-15) detected by qRT-PCR; \*,  $P < 0.05$  compared with HOK. P values were calculated using One-Way ANOVA followed by Turkey's post hoc test for multiple comparisons. Data are shown as mean  $\pm$  SD of three independent experiments.

## MiR-590-5p in OSCC via targeting RECK

associated with clinical stage ( $P < 0.001$ ), lymph node metastasis ( $P < 0.001$ ), and differentiation degree of OSCC ( $P < 0.001$ ). Particularly, those OSCC patients with higher clinical stage, lymph node metastasis or poor-/moderate differentiation had higher miR-590-5p expression.

### RECK is a target gene of miR-590-5p

To characterize the mechanism by which miR-590-5p regulates progression, we searched for potential target genes of miR-590-5p using the online bioinformatics analysis website (microRNA.org). We found the matched sequence between RECK and miR-590-5p (Fig. 2A). We were particularly interested in MMP inhibitor and tumor suppressor RECK, because in addition to its anti-invasive properties (Qin and Luo, 2014), and its lower expression was found in OSCC patients (Yuan et al., 2020). In dual luciferase reporter gene assay, the luciferase activity in the cells co-transfected with miR-590-5p mimic and RECK-WT was decreased to 0.43 times in SCC-15 ( $P = 0.001$ ) and 0.41 times in OEC-M1 ( $P < 0.001$ ) cells when compared with cells in the mimic-NC group, while SCC-15 ( $P = 0.852$ ) and OEC-M1 ( $P = 0.766$ ) cells co-transfected with miR-590-5p mimic and RECK-MUT showed no obvious difference in luciferase activity ( $P > 0.05$ , Fig. 2B,C). The result proved that RECK is a target gene of miR-590-5p.

### MiR-590-5p increased proliferation and decreased apoptosis of OSCC cells

By comparison with Mock group, miR-590-5p

inhibitor group had decreased cell proliferation (SCC-15:  $P < 0.001$ ; OEC-M1:  $P < 0.001$ ) and more than 3-fold increased cell apoptosis rate (SCC-15:  $P < 0.001$ ; OEC-M1:  $P < 0.001$ ), while si-RECK group showed significantly enhanced cell proliferation (SCC-15:  $P = 0.004$ ; OEC-M1:  $P < 0.001$ ) and about 2-fold decreased cell apoptosis rate in SCC-15 and OEC-M1 cells (Fig. 3). Compared with miR-590-5p inhibitor group, miR-590-5p inhibitor + si-RECK group was elevated in proliferative ability (SCC-15:  $P < 0.001$ ; OEC-M1:  $P < 0.001$ ) and more than 3-fold reduced in cell apoptosis rate (SCC-15:  $P < 0.001$ ; OEC-M1:  $P = 0.003$ ).

### MiR-590-5p promoted migration and invasive of OSCC cells

Wound-healing assay and Transwell invasion assay were carried out for the measurement of cell migration and invasion after transfection (Figure 4). Compared with cells in Mock group, SCC-15 and OEC-M1 cells in miR-590-5p inhibitor group decreased remarkably regarding migration (SCC-15: 0.49 fold,  $P = 0.006$ ; OEC-M1: 0.48 fold,  $P = 0.008$ ) and invasive abilities (SCC-15: 0.50 fold,  $P = 0.002$ ; OEC-M1: 0.49 fold,  $P = 0.001$ ), while si-RECK group demonstrated enhanced cell migration (SCC-15: 1.93 fold,  $P = 0.016$ ; OEC-M1: 1.88 fold,  $P = 0.016$ ) and invasion (SCC-15: 1.55 fold,  $P = 0.002$ ; OEC-M1: 1.51 fold,  $P = 0.003$ ). Besides, cells in the miR-590-5p inhibitor + si-RECK group showed apparently more obvious migration (SCC-15: 1.17 fold,  $P = 0.003$ ; OEC-M1: 2.15 fold,  $P = 0.006$ ) and invasion (SCC-15: 1.97 fold,  $P = 0.001$ ; OEC-M1: 1.95 fold,  $P = 0.002$ ) than cells of miR-590-5p inhibitor group.

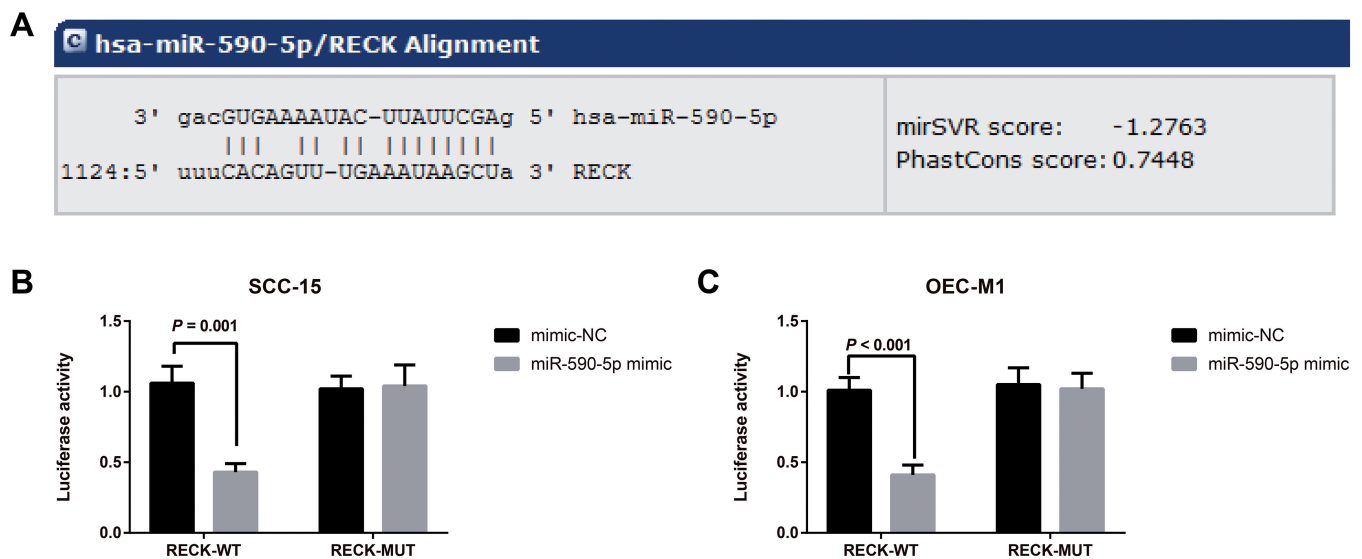


**Fig. 2.** RECK is a target gene of miR-590-5p. **A.** Binding site between RECK and miR-590-5p analyzed by using online bioinformatics analysis website microRNA.org (mirSVR score = -1.2763; PhastCons score = 0.7448); **B-C.** The dual luciferase reporter assay revealed that the luciferase activity controlled by RECK 3'-UTR was inhibited by miR-590-5p mimic in SCC-15 (**B**) and OEC-M1 (**C**) cells. P values were calculated using Student's t-test. Data represent the mean  $\pm$  SD of three independent experiments.

MiR-590-5p in OSCC via targeting RECK

Expression of miR-590-5p and RECK in transfected OSCC cells

In order to investigate the potential mechanism of miR-590-5p involving in invasion and apoptosis, western blotting were applied to analyze the protein changes of the apoptosis-related molecules (Bax and

Bcl-2) and the marker of invasion (MMP-9) (Fig. 5). Compare with SCC-15 and OEC-M1 cells in Mock group, those in miR-590-5p inhibitor group decreased strikingly in tht expressions of miR-590-5p (SCC-15: 0.39 fold, P<0.001; OEC-M1: 0.41 fold, P<0.001), Bcl-2/Bax (SCC-15: 0.20, P<0.001; OEC-M1: 0.15 fold, P<0.001) and MMP-9 (SCC-15: 0.31 fold, P=0.002;

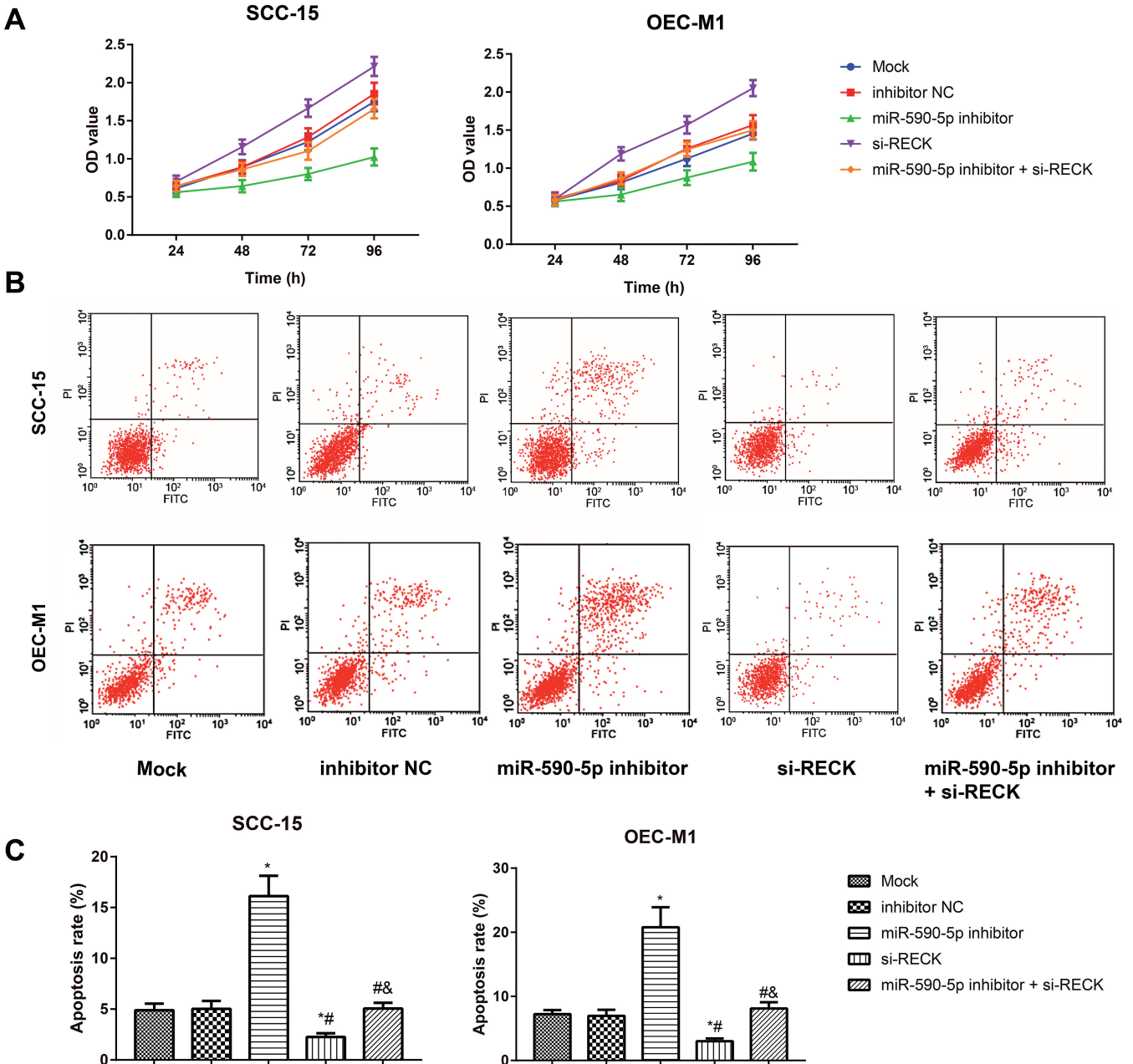


**Fig. 3.** Inhibition of miR-590-5p decreased proliferation and increased the apoptosis of OSCC cells via targeting RECK. **A.** Effect of miR-590-5p on SCC-15 and OEC-M1 cell proliferation evaluated by MTT assay; **B-C.** Effect of miR-590-5p on SCC-15 and OEC-M1 cell apoptosis detected by flow cytometry; \*, P<0.05 compared with Mock group; #, P<0.05 compared with miR-590-5p inhibitor group; &, P<0.05 compared with si-RECK group. P values were calculated using One-Way ANOVA followed by Turkey's post hoc test for multiple comparisons. Data are shown as means ± SD of three independent experiments.

MiR-590-5p in OSCC via targeting RECK

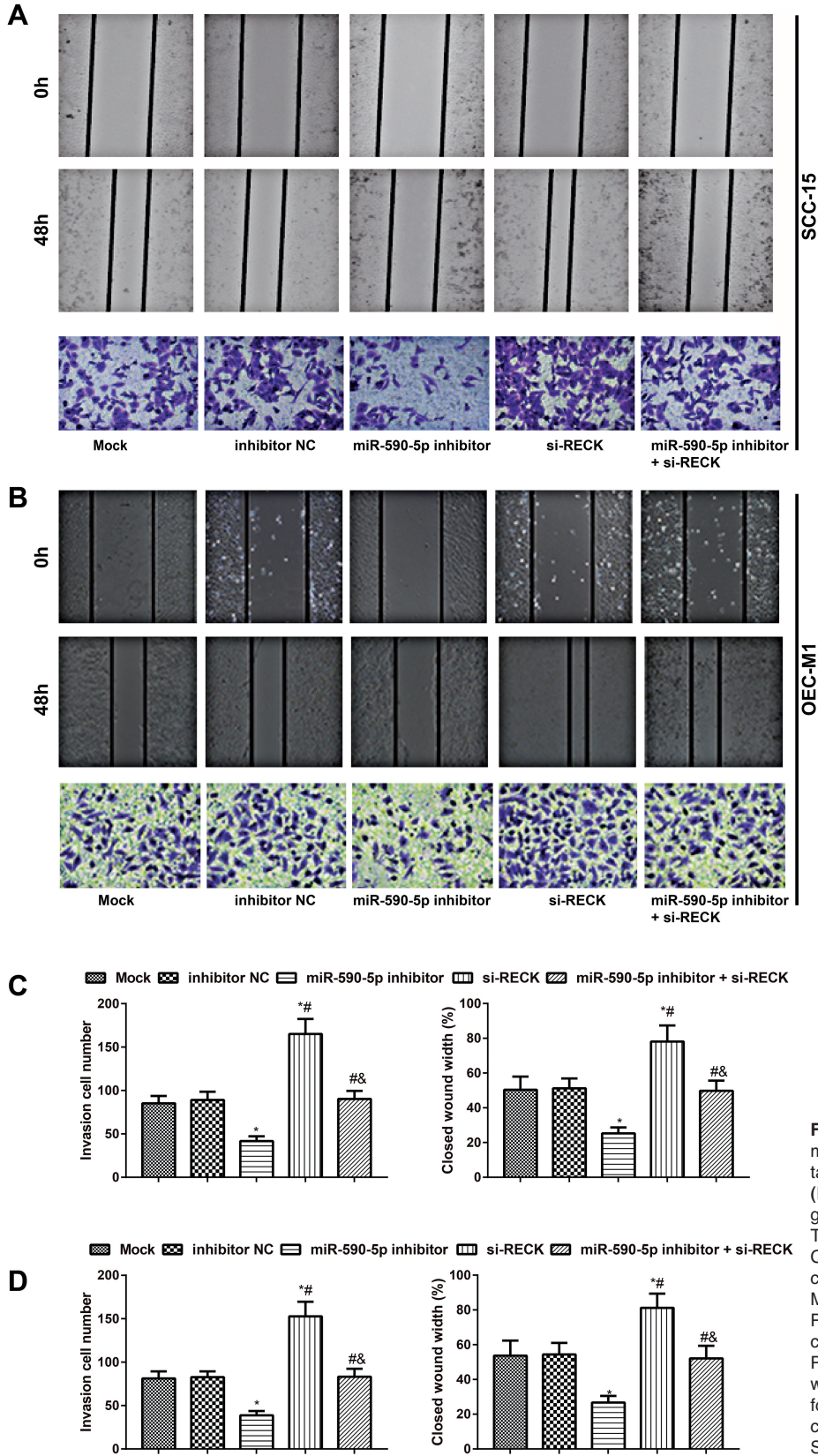


**Fig. 4.** Inhibition of miR-590-5p reduced migration and invasion of OSCC cells via targeting RECK. **A-B.** SCC-15 (**A**) and OEC-M1 (**B**) cell migration and invasive ability in each group evaluated by wound-healing and Transwell assay, respectively. **C-D.** Quantification of invasion cell number and closed wound width of SCC-15 (**C**) and OEC-M1 (**D**) cells in each transfection group; \*,  $P < 0.05$  compared with Mock group; #,  $P < 0.05$  compared with miR-590-5p inhibitor group; &,  $P < 0.05$  compared with si-RECK group. P values were calculated using One-Way ANOVA followed by Turkey's post hoc test for multiple comparisons. Data are presented as mean  $\pm$  SD of three independent experiments.

MiR-590-5p in OSCC via targeting RECK

OEC-M1: 0.29 fold,  $P < 0.001$ ), and increased greatly in the expression of RECK (SCC-15: 3.23 fold,  $P < 0.001$ ; OEC-M1: 3.20 fold,  $P < 0.001$ ). By contrast, si-RECK

group didn't show obvious change in miR-590-5p expression (SCC-15:  $P = 0.469$ ; OEC-M1:  $P = 0.720$ ), with declined RECK expression (SCC-15: 0.38 fold,

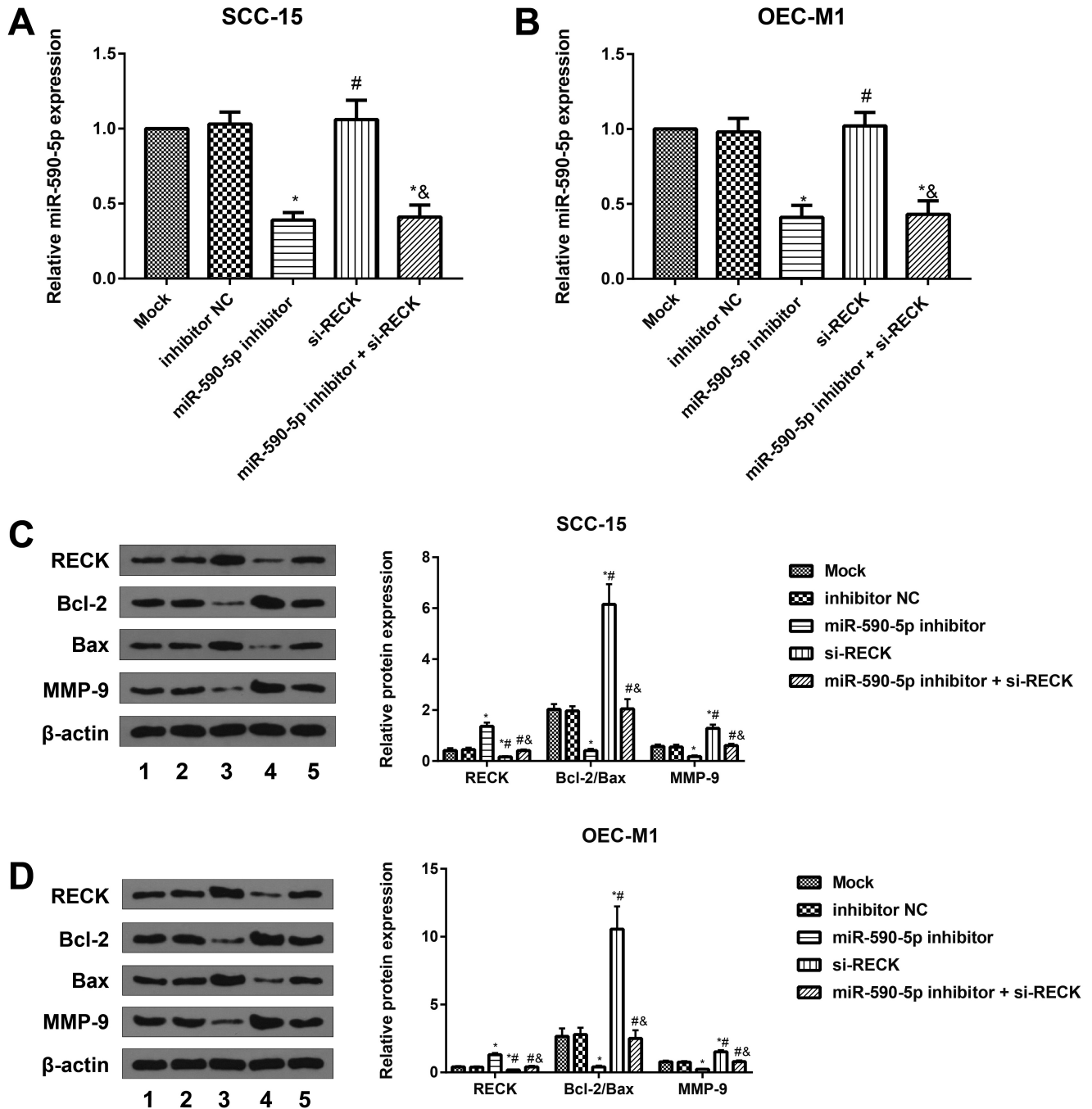


**Fig. 5.** Expression of miR-590-5p and RECK in each transfected OSCC cells. **A-B.** The expression of miR-590-5p quantified by qRT-PCR in SCC-15 (**A**) and OEC-M1 (**B**) cells. **C-D.** Protein expression of RECK, apoptosis-related molecules (Bax and Bcl-2) and the marker of invasion (MMP-9) detected by Western blotting in SCC-15 (**C**) and OEC-M1 (**D**) cells; 1, Mock group, 2, inhibitor NC group, 3, miR-590-5p inhibitor group, 4, si-RECK group, 5, miR-590-5p inhibitor + si-RECK group; \*,  $P < 0.05$  compared with Mock group; #,  $P < 0.05$  compared with miR-590-5p inhibitor group; &,  $P < 0.05$  compared with si-RECK group. P values were calculated using One-Way ANOVA followed by Turkey's post hoc test for multiple comparisons. Results were pooled from three independent experiments. Values were shown as mean  $\pm$  SD.



## MiR-590-5p in OSCC via targeting RECK

P=0.006; OEC-M1: 0.44 fold, P=0.004), as well as increased Bcl-2/Bax (SCC-15: 3.03 fold, P=0.001; OEC-M1: 3.99 fold, P=0.004) and MMP-9 expression (SCC-15: 2.21 fold, P=0.002; OEC-M1: 1.95 fold, P=0.001). In comparison with miR-590-5p inhibitor group, cells in miR-590-5p inhibitor + si-RECK group were not significantly different regarding miR-590-5p expression (SCC-15: P=0.732; OEC-M1: P=0.788), but were obviously down-regulated in RECK levels (SCC-15: 0.30 fold, P<0.001; OEC-M1: 0.31 fold, P<0.001), and markedly up-regulated in Bcl-2/Bax (SCC-15: 5 fold, P<0.001; OEC-M1: 6.10 fold, P<0.001) and MMP-9 levels (SCC-15: 3.39 fold, P=0.002; OEC-M1: 3.43 fold, P<0.001).

### Discussion

In this study, we measured the miR-590-5p expression level in OSCC tissues and cell lines. As a result, we observed an apparent up-regulation of miR-590-5p in OSCC and the close association between miR-590-5p up-regulation and the clinical TNM stage, tumor differentiation and lymph node metastasis of patients. After reviewing the published literature, a similar expression pattern of miR-590-5p was also demonstrated in other tumors. For instance, a study reported the rising expression of miR-590-5p in hepatocellular carcinoma (HCC) tissues and HCC cells, whereas down-regulation of miR-590-5p posed restrictions on the growth, migration and invasion of HCC cells (Jiang et al., 2012). Similarly in vulvar squamous cell carcinoma, the up-regulation of miR-590-5p could promote cellular malignant behaviors via its target gene *TGF $\beta$ R2* (Yang and Wu, 2016). More importantly, miR-590-5p expression was up-regulated while RECK expression was down-regulated in hypoxia-induced colorectal cancer (CRC) (Kim et al., 2018). As we know, hypoxia can induce the cancer progression and promote the metastasis potential of tumor cells (Lin et al., 2014). Given the above, we speculated that hypoxia-induced miR-590-5p up-regulation can act as an oncogene in OSCC to further influence the tumor progression.

In addition, SCC-15 and OEC-M1 cell lines were next chosen to perform the transfection experiments *in vitro*. According to the results, OSCC and OEC-M1 cells were apparently inhibited in growth, invasion and migration, but greatly advanced in apoptosis, accompanied by down-regulated miR-590-5p expression. In the meantime, silencing RECK led to completely opposite results. Similarly, a previous study also reported the increased proliferation and invasion of breast cancer cells by miR-96 via targeted down-regulation of RECK (Zhang et al., 2014). Besides, over-expressed miR-590-5p can enhance the cervical cancer cell growth by targeted regulation of *CHL1* (Chu et al., 2014). In clear cell renal carcinoma (ccRCC), miRNA-590-5p was also highly expressed and it can enhance the proliferative and invasive abilities of ccRCC by targeted regulation of PBRM1 (Xiao et al., 2013). The above

evidence suggested that inhibiting miR-590-5p can suppress the OSCC cell growth, but RECK knock-out can promote the tumor progression. However, a study indicated that miR-590-5p may function as a tumor suppressor to inhibit the proliferation of tongue cancer cells (SCC3) by targeting *FasL*, which increased the sensitivity of tongue cancer cells to the chemotherapeutic agent cisplatin (Xu et al., 2017). In contrast, the plasma-expression levels of miR-590-5p were down-regulated in head and neck cancer patients after radiotherapy (Nowicka et al., 2019). This may be a result that the functions of miR-590-5p may vary in different types of OSCC cells with different anatomy, etiology and function. Therefore, the detailed mechanisms regarding how miR-590-5p functions in conflicting ways in different OSCC cells warrant further investigation. Moreover, it is worth mentioning that RECK can be directly targeted by miRNA-590-5p, which is supported by the result of dual luciferase reporter gene assay performed in our study. And si-RECK can reverse the pro-proliferation effect of miR-590-5p inhibitor on OSCC cells. Actually, a previous study also reported that miR-221 can enhance the invasive and migration abilities of CRC cells via targeted down-regulation of RECK (Qin and Luo, 2014). Consistently, the growth and invasion of gastric cancer cells can be enhanced by miR-590-5p in line with the modulation of RECK and AKT/ERK pathway (Shen et al., 2016), indicating that miRNA-590-5p plays its regulatory role in OSCC through targeted regulation of RECK.

Furthermore, our study also revealed that miR-590-5p inhibitor can reduce the expression of miR-590-5p, Bcl-2/Bax and MMP-9, and elevate the expression of RECK, while si-RECK up-regulated the expression of Bcl-2/Bax and MMP-9, and down-regulated the expression of RECK. To our knowledge, the anti-apoptotic protein Bcl-2 and the pro-apoptotic protein Bax are two major members of Bcl-2 family, which can form homodimer or heterodimer to regulate the cell apoptosis (Spampanato et al., 2012). Besides, matrix metalloproteinase (MMPs) are the major enzymes for degradation of extracellular matrix (ECM) and they are able to degrade almost all components of ECM (Decock et al., 2011), which could damage the connective tissue matrix to cause tumor invasion, as well as tumor blood and lymph metastasis through the interaction between tumor cells and ECM (Sund et al., 2004; Fink and Boratynski, 2012). RECK is a newly discovered MMPs inhibitor and it has been proven that RECK can inhibit the expression of many MMPs, such as MT1-MMP, MMP-2 and MMP-9, at the post-transcription level, thus affecting ECM degradation, tumor invasion, metastasis and neovascularization (Noda et al., 2003; Meng et al., 2008). And there was evidence supporting that anti-miR-590-5p can improve the Caspase-3 activity and the Bax/Bcl-2 ratio and reduce the MMP-9 level in renal cell carcinoma (RCC), thereby inhibiting the growth, invasion and migration and promoting apoptosis of RCC

cells (Wang et al., 2017). Previous evidences suggested that up-regulated RECK can limit the expressions of MMP-2 and MMP-9 to inhibit OSCC proliferation and invasion (Kato et al., 2008). Furthermore, over-expressed RECK can activate the p53 signaling pathway and improve the Bax/Bcl level to enhance cervical cancer cell apoptosis and inhibit cell invasion and migration (Liu et al., 2018). Still another study reported that RECK can limit the metastasis and growth of lung cancer cells via inhibition of MMP-9 activity (Chang et al., 2008). As reported, RECK is also attributed to control Wnt/ $\beta$ -catenin signaling and mediate MMP-9 promoter activity through binding kappa B sites (Matsuzaki et al., 2018). Previous studies have shown that Wnt/ $\beta$ -catenin pathway is crucial for the tumorigenicity and invasion (Lo et al., 2018). In cancer cells, the Wnt pathway is usually activated causing  $\beta$ -catenin to accumulate in the cytoplasm and moves into the nucleus, where it binds to the TCF/LEF for transcriptional activation of downstream genes, such as cyclinD1, c-myc and MMPs (Ahmad et al., 2011). A previous study demonstrated that CRMP2 could interact with RECK, stabilized RECK expression and sequentially blocked Wnt and NF- $\kappa$ B signaling to decrease the expression of MMP-2 and MMP-9, thus inhibiting cell invasion (Lin et al., 2020). These results suggested that RECK can crosstalk with Wnt and NF- $\kappa$ B pathways to regulate signal transmission, and transcriptionally regulates the pathway target genes regulating tumorigenesis (Ma and Hottiger, 2016). In the light of these findings, it is well-grounded to believe that inhibiting miR-590-5p expression can regulate RECK expression to affect the expression of apoptosis- and invasion-related proteins, thereby inhibiting OSCC cell growth and metastasis and expediting OSCC cell apoptosis.

To conclude, our study found obvious up-regulation of miR-590-5p expression in OSCC. Besides, inhibiting miR-590-5p can lead to the up-regulation of RECK and thus the inhibition of cell proliferation, migration and invasion and the promotion of OSCC apoptosis. This novel miR-590-5p/RECK axis provides greater insight into the mechanism of OSCC development.

*Acknowledgements.* The authors appreciate the reviewers for their useful comments in this paper.

*Funding.* There was no funding in this study.

*Competing interests.* The authors declare that they have no competing interests.

## References

- Ahmad I., Morton J.P., Singh L.B., Radulescu S.M., Ridgway R.A., Patel S., Woodgett J., Winton D.J., Taketo M.M., Wu X.R., Leung H.Y. and Sansom O.J. (2011). Beta-catenin activation synergizes with pten loss to cause bladder cancer formation. *Oncogene* 30, 178-189.
- Amtha R., Razak I.A., Basuki B., Roeslan B.O., Gautama W., Puwanto D.J., Ghani W.M. and Zain R.B. (2014). Tobacco (kretek) smoking, betel quid chewing and risk of oral cancer in a selected jakarta population. *Asian Pacific journal of cancer prevention. Asian Pac. J. Cancer Prev.* 15, 8673-8678.
- Cai W., Xu Y., Yin J., Zuo W. and Su Z. (2018). Mir5905p suppresses osteosarcoma cell proliferation and invasion via targeting KLF5. *Mol. Med. Rep.* 18, 2328-2334.
- Chang C.K., Hung W.C. and Chang H.C. (2008). The Kazal motifs of RECK protein inhibit MMP-9 secretion and activity and reduce metastasis of lung cancer cells in vitro and in vivo. *J. Cell Mol. Med.* 12, 2781-2789.
- Chu Y., Ouyang Y., Wang F., Zheng A., Bai L., Han L., Chen Y. and Wang H. (2014). MicroRNA-590 promotes cervical cancer cell growth and invasion by targeting CHL1. *J. Cell Biochem.* 115, 847-853.
- Decock J., Thirkettle S., Wagstaff L. and Edwards D.R. (2011). Matrix metalloproteinases: Protective roles in cancer. *J. Cell Mol. Med.* 15, 1254-1265.
- Feng X., Luo Q., Wang H., Zhang H. and Chen F. (2018). MicroRNA-22 suppresses cell proliferation, migration and invasion in oral squamous cell carcinoma by targeting NLRP3. *J. Cell Physiol.* 233, 6705-6713.
- Fink K. and Boratynski J. (2012). The role of metalloproteinases in modification of extracellular matrix in invasive tumor growth, metastasis and angiogenesis. *Postepy Hig Med. Dosw (Online)* 66, 609-628 (in Polish).
- Gombos K., Horvath R., Szele E., Juhasz K., Gocze K., Somlai K., Pajkos G., Ember I. and Olasz L. (2013). MiRNA expression profiles of oral squamous cell carcinomas. *Anticancer Res.* 33, 1511-1517.
- Jerjes W., Upile T., Petrie A., Riskalla A., Hamdoon Z., Vourvachis M., Karavidas K., Jay A., Sandison A., Thomas G.J., Kalavrezos N. and Hopper C. (2010). Clinicopathological parameters, recurrence, locoregional and distant metastasis in 115 t1-t2 oral squamous cell carcinoma patients. *Head Neck Oncol.* 2, 9.
- Jiang X., Xiang G., Wang Y., Zhang L., Yang X., Cao L., Peng H., Xue P. and Chen D. (2012). MicroRNA-590-5p regulates proliferation and invasion in human hepatocellular carcinoma cells by targeting TGF-beta RII. *Mol. Cells.* 33, 545-551.
- Kato K., Long N.K., Makita H., Toida M., Yamashita T., Hatakeyama D., Hara A., Mori H. and Shibata T. (2008). Effects of green tea polyphenol on methylation status of reck gene and cancer cell invasion in oral squamous cell carcinoma cells. *Br J. Cancer* 99, 647-654.
- Kim C.W., Oh E.T., Kim J.M., Park J.S., Lee D.H., Lee J.S., Kim K.K. and Park H.J. (2018). Hypoxia-induced microrna-590-5p promotes colorectal cancer progression by modulating matrix metalloproteinase activity. *Cancer Lett.* 416, 31-41.
- Li X.Y., Luo Q.F., Wei C.K., Li D.F., Li J. and Fang L. (2014). MiRNA-107 inhibits proliferation and migration by targeting CDk8 in breast cancer. *Int. J. Clin. Exp. Med.* 7, 32-40.
- Lin S.C., Liao W.L., Lee J.C. and Tsai S.J. (2014). Hypoxia-regulated gene network in drug resistance and cancer progression. *Exp. Biol. Med. (Maywood)* 239, 779-792.
- Lin B., Li Y., Wang T., Qiu Y., Chen Z., Zhao K. and Lu N. (2020). CRMP2 is a therapeutic target that suppresses the aggressiveness of breast cancer cells by stabilizing RECK. *Oncogene.* 39, 6024-6040.
- Liu L.T., Chang H.C., Chiang L.C. and Hung W.C. (2003). Histone deacetylase inhibitor up-regulates reck to inhibit MMP-2 activation

## MiR-590-5p in OSCC via targeting RECK

- and cancer cell invasion. *Cancer Res.* 63, 3069-3072.
- Liu Y., Li L., Liu Y., Geng P., Li G., Yang Y. and Song H. (2018). RECK inhibits cervical cancer cell migration and invasion by promoting p53 signaling pathway. *J. Cell Biochem.* 119, 3058-3066.
- Lo R.C., Leung C.O., Chan K.K., Ho D.W., Wong C.M., Lee T.K. and Ng I.O. (2018). Cripto-1 contributes to stemness in hepatocellular carcinoma by stabilizing dishevelled-3 and activating wnt/beta-catenin pathway. *Cell Death Differ.* 25, 1426-1441.
- Long N.K., Kato K., Yamashita T., Makita H., Toida M., Hatakeyama D., Hara A., Mori H. and Shibata T. (2008). Hypermethylation of the RECK gene predicts poor prognosis in oral squamous cell carcinomas. *Oral Oncol.* 44, 1052-1058.
- Ma B. and Hottiger M.O. (2016). Crosstalk between wnt/beta-catenin and NF-kappaB signaling pathway during inflammation. *Front. Immunol.* 7, 378.
- Matsuzaki T., Kitayama H., Omura A., Nishimoto E., Alexander D.B. and Noda M. (2018). The RECK tumor-suppressor protein binds and stabilizes ADAMTS10. *Biol. Open.* 7, bio033985.
- Meng N., Li Y., Zhang H. and Sun X.F. (2008). RECK, a novel matrix metalloproteinase regulator. *Histol. Histopathol.* 23, 1003-1010.
- Noda M., Oh J., Takahashi R., Kondo S., Kitayama H. and Takahashi C. (2003). RECK: A novel suppressor of malignancy linking oncogenic signaling to extracellular matrix remodeling. *Cancer Metastasis Rev.* 22, 167-175.
- Nowicka Z., Stawiski K., Tomasik B. and Fendler W. (2019). Extracellular mirnas as biomarkers of head and neck cancer progression and metastasis. *Int. J. Mol. Sci.* 20.
- Qin J. and Luo M. (2014). MicroRNA-221 promotes colorectal cancer cell invasion and metastasis by targeting RECK. *FEBS Lett.* 588, 99-104.
- Shen B., Yu S., Zhang Y., Yuan Y., Li X., Zhong J. and Feng J. (2016). Mir-590-5p regulates gastric cancer cell growth and chemosensitivity through RECK and the AKT/ERK pathway. *Onco Targets Ther.* 9, 6009-6019.
- Shiah S.G., Hsiao J.R., Chang W.M., Chen Y.W., Jin Y.T., Wong T.Y., Huang J.S., Tsai S.T., Hsu Y.M., Chou S.T., Yen Y.C., Jiang S.S., Shieh Y.S., Chang I.S., Hsiao M. and Chang J.Y. (2014). Downregulated mir329 and mir410 promote the proliferation and invasion of oral squamous cell carcinoma by targeting wnt-7b. *Cancer Res.* 74, 7560-7572.
- Spampanato C., De Maria S., Sarnataro M., Giordano E., Zanfardino M., Baiano S., Carteni M. and Morelli F. (2012). Simvastatin inhibits cancer cell growth by inducing apoptosis correlated to activation of bax and down-regulation of *bcl-2* gene expression. *Int. J. Oncol.* 40, 935-941.
- Sund M., Xie L. and Kalluri R. (2004). The contribution of vascular basement membranes and extracellular matrix to the mechanics of tumor angiogenesis. *APMIS* 112, 450-462.
- Wang L., Wei W.Q., Wu Z.Y. and Wang G.C. (2017). MicroRNA-590-5p regulates cell viability, apoptosis, migration and invasion of renal cell carcinoma cell lines through targeting ARHGAP24. *Mol. Biosyst.* 13, 2564-2573.
- Weaver V.M. (2002). Membrane-associated mmp regulators: Novel cell adhesion tumor suppressor proteins?. *Dev. Cell* 2, 6-7.
- Wikner J., Grobe A., Pantel K. and Riethdorf S. (2014). Squamous cell carcinoma of the oral cavity and circulating tumour cells. *World J. Clin. Oncol.* 5, 114-124.
- Xiao X., Tang C., Xiao S., Fu C. and Yu P. (2013). Enhancement of proliferation and invasion by microRNA-590-5p via targeting PBRM1 in clear cell renal carcinoma cells. *Oncol. Res.* 20, 537-544.
- Xu M., Wang H.F. and Zhang H.Z. (2015). Expression of RECK and mmps in hepatoblastoma and neuroblastoma and comparative analysis on the tumor metastasis. *Asian Pac. J. Cancer Prev.* 16, 4007-4011.
- Xu Y., Han T., Zhu Y. and Chen Q. (2017). Mir-590-5p inhibits the progression of tongue squamous cell carcinoma by targeting FASL. *Int. J. Clin. Exp. Pathol.* 10, 11880-11887.
- Yang X. and Wu X. (2016). MiRNA expression profile of vulvar squamous cell carcinoma and identification of the oncogenic role of mir-590-5p. *Oncol. Rep.* 35, 398-408.
- Yang H., Zheng W., Zhao W., Guan C. and An J. (2013). Roles of mir-590-5p and mir-590-3p in the development of hepatocellular carcinoma. *Nan Fang Yi Ke Da Xue Xue Bao.* 33, 804-811 (in Chinese).
- Yang C.N., Deng Y.T., Tang J.Y., Cheng S.J., Chen S.T., Li Y.J., Wu T.S., Yang M.H., Lin B.R., Kuo M.Y., Ko J.Y. and Chang C.C. (2015). MicroRNA-29b regulates migration in oral squamous cell carcinoma and its clinical significance. *Oral Oncol.* 51, 170-177.
- Yuan J., Li W., Zhu J., Deng S. and Tao X. (2020). Low expression of RECK in oral squamous cell carcinoma patients induces a shorter survival rate through an imbalance of RECK/MMPS. *Int. J. Clin. Exp. Pathol.* 13, 501-508.
- Zhang J., Kong X., Li J., Luo Q., Li X., Shen L., Chen L. and Fang L. (2014). Mir-96 promotes tumor proliferation and invasion by targeting reck in breast cancer. *Oncol. Rep.* 31, 1357-1363.
- Zhang L.W., Li J., Cong X., Hu X.S., Li D., Wu L.L., Hua H., Yu G.Y. and Kerr A.R. (2018). Incidence and mortality trends in oral and oropharyngeal cancers in china, 2005-2013. *Cancer Epidemiol.* 57, 120-126.
- Zhou Q., Zhu Y., Wei X., Zhou J., Chang L., Sui H., Han Y., Piao D., Sha R. and Bai Y. (2016). Mir-590-5p inhibits colorectal cancer angiogenesis and metastasis by regulating nuclear factor 90/vascular endothelial growth factor a axis. *Cell Death Dis.* 7, e2413.